A variational approach to the perpendicular joining of nanotubes to plane sheets

2008 J. Phys. A: Math. Theor. 41 125203

(http://iopscience.iop.org/1751-8121/41/12/125203)

IOP PUBLISHING JOURNAL OF PHYSICS A: MATHEMATICAL AND THEORETICAL

J. Phys. A: Math. Theor. **41** (2008) 125203 (11pp) doi:10.1088/1751-8113/41/12/125203

A variational approach to the perpendicular joining of nanotubes to plane sheets

Barry J Cox and James M Hill

Nanomechanics Group, School of Mathematics and Applied Statistics, University of Wollongong, Wollongong, NSW 2522, Australia

E-mail: barryc@uow.edu.au

Received 21 December 2007, in final form 13 February 2008
Published 10 March 2008
Online at stacks.iop.org/JPhysA/41/125203

Abstract

The design of many novel electronic devices will hinge on our understanding of the joining of certain nanostructures. In particular, the perpendicular joining of a carbon nanotube to a flat graphene sheet applies to the situation of connecting to an electronic platform. Connecting carbon nanostructures essentially involves a discrete geometric procedure, and the present authors have attempted to solve such problems by invoking the principle that the bond lengths and bond angles at the join are determined in such a manner that their total squared deviation from some ideal configuration is a minimum. Other authors suggest that carbon nanotubes might be deformed in such a way that their total curvature squared is minimized. From a theoretical standpoint, any continuous approach to such essentially discrete problems could be a valuable tool in obtaining the main qualitative features at the join. Here we propose a continuous variational approach to the determination of the join geometry assuming that the curvature is minimized for prescribed join lengths and defect geometries. We find that the variational model provides good overall agreement with the least-squares method in terms of the nanotube attachment height. Although the agreement in participating atomic positions is not quite as good, the absolute error in the positioning of participating atoms is less than 0.18 Å. Current experimental data does not exist to determine which procedure gives the more realistic results.

PACS numbers: 02.30.Xx, 61.46.De, 81.05.Uw

1. Introduction

In Baowan *et al* [1] a numerical method is proposed to determine the geometric parameters for joins between right circular cylindrical carbon nanotubes and planar graphene sheets. The method is based on a discrete model for the carbon atoms and the covalent bonds comprising

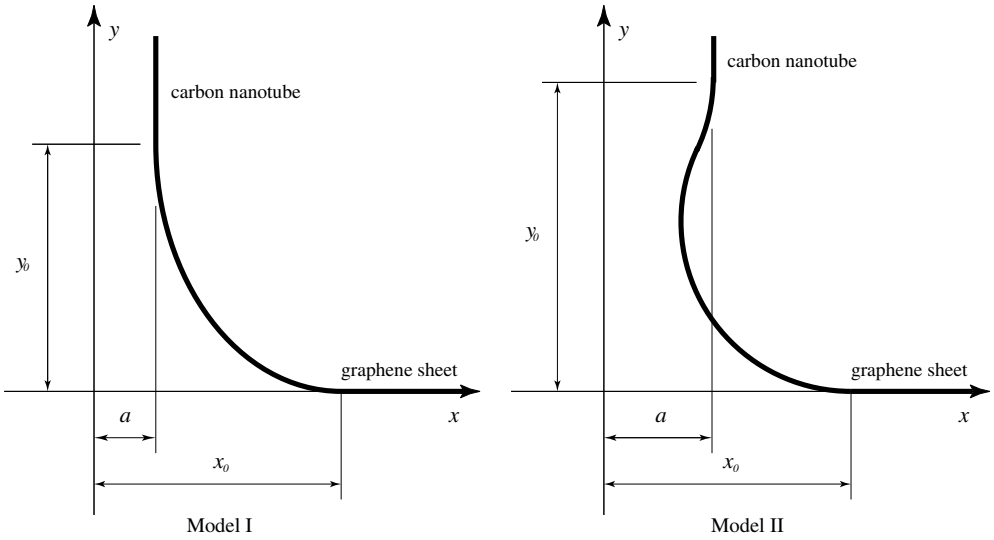

Figure 1. The problem geometries for Model I, in which the join contains only positive curvature, and Model II, which has both positive and negative curvatures in the join region.

the join, and the particular geometries that are generated, are obtained by the principle of minimizing the difference of the square of the distance between atoms which are separated by two covalent bonds and their maximum possible distance. The discrete geometric method proposed by Baowan *et al* [1] is related to certain bonded potential energy methods as proposed by Cornell *et al* [2], Li and Chou [3], Jin and Yuan [4] and Natsuki *et al* [5]. Either approach involves substantial numerical computation, and the question arises, 'to what extent can such intrinsically discrete models be approximated by a continuous model?' Any continuous model which accounts for the dominant qualitative features of the discrete models would, from a theoretical perspective, be highly desirable. In a recent paper, Zang *et al* [6], these authors propose that carbon nanotubes under pressure can be modelled by minimizing the curvature squared, and bearing in mind that the bonded potential energy relates to the elastic bending energy from small deformation elastic theory, here we also follow such an approach.

In the present paper, we also consider a continuous approach to this problem and use variational calculus to determine the curve adopted by a line connecting a horizontal plane and vertical carbon nanotube, such that the arc length of the curve and the size of the defect in the graphene sheet are specified. On the other hand, the distance of the cylindrical part of the carbon nanotube from the graphene sheet is not prescribed and is determined as a part of the solution.

We position the graphene sheet in the (x, z)-plane with a circular defect of radius x_0 centred on the origin. We also assume that a nanotube of radius a is located with its axis co-linear with the y-axis starting from an unknown positive distance above the (x, z)-plane which we will denote by y_0. Since the defect and the nanotube are rotationally symmetric about the y-axis, we can consider this as a problem in the two-dimensional (x, y)-plane. The connecting covalent bonds are assumed to join the points on the graphene defect $(x_0, 0)$, and the nanotube (a, y_0) and have a total prescribed arc length ℓ. Two likely configurations are illustrated in figure 1. We comment that the problem is only physically sensible if the defect edge at $x = x_0$ is within a distance given by the prescribed arc length ℓ of the tube radius,

$x = a$. That is, we require the inequalities $a - \ell < x_0 < a + \ell$ to be satisfied otherwise the problem has no solution.

In the terminology of the calculus of variations we seek to determine the function $y(x)$ which has an element of arc length $\mathrm{d}s$, such that the functional

$$J[y] = \int_0^\ell \kappa^2 \,\mathrm{d}s + \lambda \int_0^\ell \mathrm{d}s$$

is an extremum, where κ is the curvature and λ is a Lagrange multiplier corresponding to the fixed length constraint and which is used to determine the height of the nanotube y_0. For a two-dimensional curve $y = y(x)$, we have $\kappa = y''/(1+y'^2)^{3/2}$ and this equation can be shown to become

$$J[y] = \int_a^{x_0} \frac{y''^2 \,\mathrm{d}x}{(1+y'^2)^{5/2}} + \lambda \int_a^{x_0} (1+y'^2)^{1/2} \,\mathrm{d}x, \tag{1}$$

where primes throughout denote differentiation with respect to x. We consider two distinct models as shown in figure 1. One for which the join curvature remains positive, which we examine in section 3, and another for which the join comprises two regions, one of positive curvature and the other of negative curvature, which we deal with in section 4. For both models we impose the continuity boundary conditions at the graphene sheet,

$$y(x_0) = 0, \qquad y'(x_0) = 0. \tag{2}$$

The boundary conditions at the carbon nanotube are determined by integration by parts of the functional equation (1), and after applying the delta operator we may derive the standard equation

$$\delta J[y] = \left[\left(F_{y'} - \frac{\mathrm{d}}{\mathrm{d}x}F_{y''}\right)\delta y + F_{y''}\delta y'\right]_a^{x_0} + \int_a^{x_0} \left(F_y - \frac{\mathrm{d}}{\mathrm{d}x}F_{y'} + \frac{\mathrm{d}^2}{\mathrm{d}x^2}F_{y''}\right)\delta y \,\mathrm{d}x, \tag{3}$$

where subscripts denote partial derivatives and here F is given by

$$F(y', y'') = \frac{y''^2}{(1+y'^2)^{5/2}} + \lambda(1+y'^2)^{1/2}. \tag{4}$$

In the present case only y' is prescribed at $x = a$, since y_0 is unknown, and therefore at $x = a$ we require the natural or alternative boundary condition given by

$$\left(F_{y'} - \frac{\mathrm{d}}{\mathrm{d}x}F_{y''}\right)\bigg|_{x=a} = 0. \tag{5}$$

In Model I, the value of y' ranges from 0 at $x = x_0$ to $-\infty$ at $x = a$. Therefore, in Model I, the boundary condition is $y'(a) = -\infty$. In Model II, y' ranges from 0 to $-\infty$, where it changes sign and then ranges from ∞ down to some finite positive value before returning to ∞. Therefore, in Model II, the boundary condition is $y'(a) = \infty$. Thus for the two models we have at $x = a$, equation (5) along with

$$y'(a) = -\infty, \quad \text{Model I} \tag{6}$$

$$y'(a) = \infty, \quad \text{Model II} \tag{7}$$

and in both cases y_0 is determined from the value $y_0 = y(a)$. In the following section, we derive the equation

$$\kappa = \pm\left(\lambda + \frac{\alpha}{(1+y'^2)^{1/2}}\right)^{1/2}, \tag{8}$$

where α is a constant and from which we immediately note that the special case $\alpha = 0$ corresponds to a circular join with a constant curvature.

In the following section, we examine the general calculus of variations problem and then derive the appropriate Euler–Lagrange equation for the present problem. In section 3 we examine the case of a strictly positive curvature, identified as Model I in figure 1. Following this, in section 4 we extend the analysis to the case involving both the positive and negative curvatures, which we refer to as Model II. In section 5 we examine some numerical calculations based on both models, initially for some general nondimensional cases, and subsequently for the case examined in Baowan *et al* [1] by the discrete geometric method. Finally, in section 6 we present a brief conclusion to summarize the major outcomes.

2. The Euler–Lagrange equation

From (3) we observe that we have the usual Euler–Lagrange equation for those functions $F(x, y, y', y'')$, which depend on the second derivative of the function y, that is

$$F_y - \frac{\mathrm{d}}{\mathrm{d}x}F_{y'} + \frac{\mathrm{d}^2}{\mathrm{d}x^2}F_{y''} = 0. \tag{9}$$

Since here F does not depend explicitly on y we know that $F_y = 0$, and we can immediately integrate (9) to obtain

$$F_{y'} - \frac{\mathrm{d}}{\mathrm{d}x}F_{y''} = C_1,$$

where C_1 is an arbitrary constant of integration. Furthermore, we note from the alternative boundary condition (5) that at the boundary $x = a$, $C_1 = 0$ and therefore, for the entire domain we have

$$F_{y'} = \frac{\mathrm{d}}{\mathrm{d}x}F_{y''}. \tag{10}$$

Now by definition of the full derivative we have

$$\frac{\mathrm{d}}{\mathrm{d}x}F = F_x + y'F_y + y''F_{y'} + y'''F_{y''},$$

and since in this case $F_x \equiv F_y \equiv 0$, and also substituting from (10) gives

$$\frac{\mathrm{d}}{\mathrm{d}x}F = y''\frac{\mathrm{d}}{\mathrm{d}x}F_{y''} + y'''F_{y''},$$

which can be rearranged to give

$$\frac{\mathrm{d}}{\mathrm{d}x}(F - y''F_{y''}) = 0,$$

whereupon integrating with respect to x gives

$$F - y''F_{y''} = -\alpha, \tag{11}$$

where α is an arbitrary constant of integration. We now substitute from (4) into (11) from which we may obtain

$$\frac{y''^2}{(1+y'^2)^3} = \lambda + \frac{\alpha}{(1+y'^2)^{1/2}},$$

and since the left-hand side is the square of the curvature κ^2 and therefore we have derived integral (8). We first comment that since for both models, y' is zero at one endpoint and infinite at the other. Therefore, the second term in the parentheses of (8) ranges in value from 0 to α, and to maintain physical sensibility κ is real and we have that $\lambda > 0$ and $\alpha > -\lambda$. We again note that α can take a zero value, arising from $\kappa = \lambda^{1/2}$, which corresponds to the special case of a circular join with a constant curvature.

3. Model I: positive curvature

On making the substitution $\tan\theta = y'$, and assuming positive curvature, equation (8) becomes

$$\kappa = (\lambda + \alpha\cos\theta)^{1/2}, \tag{12}$$

and from the definition of curvature $\kappa = y''/(1+y'^2)^{3/2}$ and making the same substitution for y' which gives

$$\frac{\mathrm{d}y}{\mathrm{d}\theta} = \frac{\sin\theta}{(\lambda+\alpha\cos\theta)^{1/2}}.$$

Now in order to simplify later algebra we introduce the constant $k = [(\lambda+\alpha)/2\alpha]^{1/2}$ and the new parametric variable ϕ, which is defined by

$$\cos\theta = 1 - 2k^2\sin^2\phi. \tag{13}$$

It may be shown from these substitutions that

$$\frac{\mathrm{d}\theta}{\mathrm{d}\phi} = \frac{2k\cos\phi}{(1-k^2\sin^2\phi)^{1/2}},$$

and on introducing a second new constant $\beta = (2/\alpha)^{1/2}$ we may deduce

$$\frac{\mathrm{d}y}{\mathrm{d}\phi} = 2\beta k\sin\phi,$$

which on integration yields

$$y(\phi) = 2\beta k(1-\cos\phi); \tag{14}$$

noting that the constant of integration arises from the boundary conditions (2). Here we can consider (14) as a parametric equation for y in terms of the parameter ϕ, and denote the value of ϕ at the point where $\theta = -\pi/2$ with $\phi_0 = \sin^{-1}(1/\sqrt{2}k)$, and note that for Model I, $-\phi_0 < \phi \leqslant 0$.

Now we determine the corresponding parametric equation for x by taking equation (12) and substituting $\mathrm{d}y = \tan\theta\,\mathrm{d}x$, which yields

$$\frac{\mathrm{d}x}{\mathrm{d}\theta} = \frac{\cos\theta}{(\lambda+\alpha\cos\theta)^{1/2}}, \tag{15}$$

and after changing to the new parameter ϕ we obtain

$$\frac{\mathrm{d}x}{\mathrm{d}\phi} = \beta\frac{1-2k^2\sin^2\phi}{(1-k^2\sin^2\phi)^{1/2}},$$

or alternatively

$$\frac{\mathrm{d}x}{\mathrm{d}\phi} = \beta\left[2(1-k^2\sin^2\phi)^{1/2} - \frac{1}{(1-k^2\sin^2\phi)^{1/2}}\right],$$

which upon integration yields

$$x(\phi) = x_0 + \beta[2E(\phi,k) - F(\phi,k)], \tag{16}$$

where the constant of integration arises from the boundary condition (2), and $F(\phi,k)$ and $E(\phi,k)$ denote the usual Legendre incomplete elliptic integrals of the first and second kinds, respectively. We use the form of these integrals as specified in Byrd and Friedman [7].

Now from the boundary condition (6) for Model I, at the point $x = a$ where the join meets the tube, on substituting these values into (14) and (16) yields

$$y_0 = 2\beta k(1-\cos\phi_0), \tag{17}$$

$$x_0 - a = \beta[2E(\phi_0, k) - F(\phi_0, k)]. \tag{18}$$

From the arc length constraint we have

$$\ell = \int_a^{x_0} (1 + y'^2)^{1/2}\, \mathrm{d}x,$$

so that now on substituting $y' = \tan\theta$ according to (15) we have

$$\ell = \int_{-\pi/2}^{0} \frac{\mathrm{d}\theta}{(\lambda + \alpha\cos\theta)^{1/2}},$$

and the substitution $\cos\theta = 1 - 2k^2\sin^2\phi$ yields

$$\ell = \beta \int_{-\phi_0}^{0} \frac{\mathrm{d}\phi}{(1 - k^2\sin^2\phi)^{1/2}},$$

from which we may deduce

$$\ell = \beta F(\phi_0, k). \tag{19}$$

Thus, for a prescribed a, x_0 and ℓ, equations (18) and (19) constitute two equations for the determination of the two unknowns β and k from which the attachment height y_0 may be obtained from (17).

By substitution of equation (19) into equation (18), we may derive

$$\mu = 2\left(\frac{E(\phi_0, k)}{F(\phi_0, k)}\right) - 1, \tag{20}$$

where $\mu = (x_0 - a)/\ell$ and $-1 < \mu < 1$. Since $\phi_0 = \sin^{-1}(1/\sqrt{2}k)$, equation (20) must be solved numerically for a given μ, to determine the value for k, and hence ϕ_0. Then by substitution back into (19) the value of β is determined and therefore y_0 can be determined from (17).

4. Model II: positive and negative curvatures

In this section we proceed exactly as in section 3, for positive curvature, for the first region from the point of attachment to the graphene sheet $(x_0, 0)$ up until the critical point (x_c, y_c) where the curvature changes sign. We then consider the second region from the critical point (x_c, y_c) to the point of attachment to the carbon nanotube (a, y_0) throughout which the curvature is negative. We denote the value of the parameter θ as defined in the previous section at the critical point to be θ_c, and from geometrical considerations we have that $-\pi < \theta_c < -\pi/2$.

The same considerations apply to the region of positive curvature as used in section 3 and therefore equations (14) and (16) are valid in the first region of Model II. This region is bounded by the point where the curvature $\kappa = 0$, and from (12), we may derive

$$\theta_c = -\cos^{-1}(-\lambda/\alpha).$$

Now employing the new parametric variable ϕ as defined by (13), we determine that $\phi = -\pi/2$ when $\theta = \theta_c$. By substituting $\phi = -\pi/2$ into equations (14) and (16), we may derive

$$y_c = 2\beta k, \qquad x_c = x_0 - \beta[2E(k) - K(k)], \tag{21}$$

where β and k are as defined in section 3, and $K(k)$ and $E(k)$ are the usual complete elliptic integrals of the first and second kinds, respectively.

In the second region, we take the negative sign of (8) and following a similar procedure to that described in section 3 gives

$$y(\phi) = 2\beta k(1 + \cos\phi), \tag{22}$$

where the constant of integration arises from the condition that $y = y_c$ when $\phi = -\pi/2$ and then we use expression (21) for y_c. We note that equation (22) differs from (14) only by a change in the sign of one term. Similarly, by taking the negative sign of (8) and solving for the parametric form of x we may derive

$$x(\phi) = 2x_c - x_0 - \beta[2E(\phi, k) - F(\phi, k)],$$

where the constant of integration is determined from the boundary condition at $\phi = -\pi/2$. On substituting for x_c using (21) yields

$$x(\phi) = x_0 - \beta\{2[2E(k) - E(-\phi, k)] - [2K(k) - F(-\phi, k)]\}, \tag{23}$$

and we comment that throughout we follow the usual convention that $E(k)$ refers to the complete elliptic integral of the second kind while $E(-\phi, k)$ denotes the corresponding incomplete elliptic integral.

Now from the boundary conditions at the point of attachment to the carbon nanotube (7) we know that $\phi = -\phi_0$ at the point (a, y_0). By substitution into (22) we may derive

$$y_0 = 2\beta k(1 + \cos\phi_0), \tag{24}$$

and similarly, substitution in (23) gives

$$x_0 - a = \beta\{2[2E(k) - E(\phi_0, k)] - [2K(k) - F(\phi_0, k)]\}. \tag{25}$$

The arc length constraint is obtained from the two regions and we have

$$\ell = \int_{\theta_c}^{0} \frac{\mathrm{d}\theta}{(\lambda + \alpha\cos\theta)^{1/2}} + \int_{\theta_c}^{-\pi/2} \frac{\mathrm{d}\theta}{(\lambda + \alpha\cos\theta)^{1/2}},$$

which by essentially the same procedure to that employed in section 3 we may derive

$$\ell = \beta[2K(k) - F(\phi_0, k)]. \tag{26}$$

Thus for a prescribed a, x_0 and ℓ, equations (25) and (26) constitute two equations for the two unknowns β and k, remembering that $\phi_0 = \sin^{-1}(1/\sqrt{2}k)$. Once these two constants are determined, the attachment height y_0 may be obtained from (24).

By straightforward algebra we may deduce

$$\mu = 2\left(\frac{2E(k) - E(\phi_0, k)}{2K(k) - F(\phi_0, k)}\right) - 1, \tag{27}$$

where as before, $\mu = (x_0 - a)/\ell$. Since $\phi_0 = \sin^{-1}(1/\sqrt{2}k)$, equation (27) only involves the single unknown k. We may solve this equation numerically for a prescribed μ, to determine the value for k which in turn gives the value for ϕ_0. By further substitution into (26) gives the value for β, which allows, by substitution into (24), the attachment height y_0 to be deduced.

We observe that formally equation (20) coincides with (27) for the value $k = 1/\sqrt{2}$. We denote the value of μ at this point by μ_0 and we have

$$\mu_0 = 2\left(\frac{E(1/\sqrt{2})}{K(1/\sqrt{2})}\right) - 1 = 0.456\,946\,5810\ldots, \tag{28}$$

where $K(k)$ and $E(k)$ are the complete elliptic integrals of the first and second kinds, respectively.

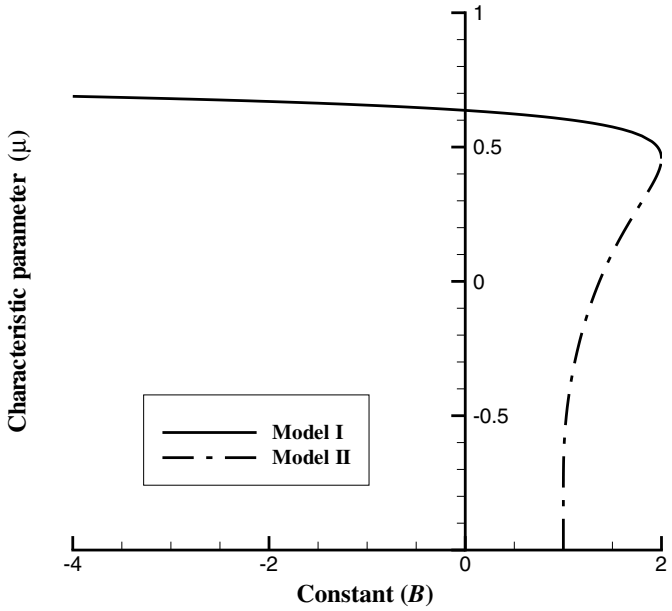

Figure 2. Relation between the characteristic parameter $\mu = (x_0 - a)/\ell$ and constant $B = 1/k^2$ for both models, obtained from (20) and (27).

5. Numerical results

We begin by examining some general features of the solutions to Models I and II, and then subsequently examine a particular carbon nanotube–graphene join.

The first observation is that the solution is characterized by the nondimensional characteristic parameter $\mu = (x_0 - a)/\ell$. The different regions of the solution can be seen by examining equations (20) and (27) as shown in figure 2 which for convenience we plot μ against a new constant $B = 1/k^2$. In this plot three distinct regions are evident. First there is the region $2/\pi < \mu < 1$, which corresponds to joins with arc length ℓ, less than a quarter of a circle circumference of radius $x_0 - a$. In this case the constant B is negative, which corresponds to a negative value of α and an imaginary modulus k for the elliptic integrals. The solution asymptotes with the line $\mu = 1$, and crosses the vertical axis at the point $\mu = 2/\pi$, which corresponds to the solution degenerating to a constant curvature (i.e. a circular join). The second region exists for $\mu_0 \leqslant \mu < 2/\pi$, where μ_0 is given in (28), and corresponds to Model I when the arc length ℓ of the join is greater than the quarter circumference of a circle of radius $x_0 - a$. In this region $0 < B \leqslant 2$, and therefore α is always positive and the modulus k is strictly real. The third and final region applies to the range $-1 < \mu < \mu_0$, and corresponds to Model II. This model is invoked when the arc length ℓ, is much greater than the quarter circumference of a circle of radius $x_0 - a$, and therefore a change of curvature is necessary to accommodate the join. For Model II, the constant B is restricted to the range $1 < B \leqslant 2$ and therefore again α is strictly positive. As can be seen from figure 2, the constant B never takes a value greater than 2 for any of the solution regions.

We now apply the solutions derived in sections 3 and 4 to a nondimensionalized situation. We assume a fixed arc length $\ell = 1$ and a graphene attachment point $x_0 = 1$. We then allow the tube radius a, to take values between 0.1 and 0.9, in increments of 0.1. In this configuration

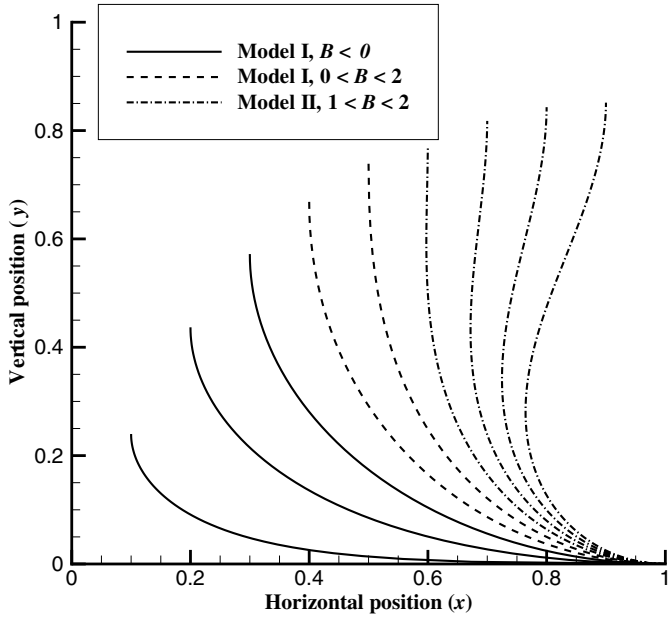

Figure 3. Nondimensional plots of joins $y = y(x)$ for various values of μ.

Table 1. Numerical values for the parameter μ, corresponding constant k and attachment height y_0 for various tube radii a assuming $x_0 = \ell = 1$.

a	μ	Model	k	y_0
0.1	0.9	I	0.004 739 80i	0.239 857 78
0.2	0.8	I	0.099 135 84i	0.436 837 09
0.3	0.7	I	0.421 216 51i	0.572 073 31
0.4	0.6	I	0.954 637 59	0.668 386 32
0.5	0.5	I	0.714 165 31	0.738 729 74
0.6	0.4	II	0.714 228 72	0.789 576 89
0.7	0.3	II	0.744 140 01	0.824 438 60
0.8	0.2	II	0.781 018 61	0.845 295 25
0.9	0.1	II	0.818 760 73	0.853 212 08

$\mu = 1 - a$, and the resulting joins are shown in figure 3. As can be seen from this figure, for the three cases when $2/\pi < \mu < 1$, Model I is used with a negative value of $1/k^2$. For the cases when $\mu_0 < \mu < 2/\pi$, Model I is again used, however in these cases $0 < 1/k^2 < 2$. Finally, the cases when $-1 < \mu < \mu_0$, Model II provides the solution. For various values of the characteristic parameter μ, numerical values of the constant k and the attachment height y_0 for all the curves in the figure are listed in table 1.

We now compare our results with those of Baowan *et al* [1] who examine the symmetric join for a (6,0) nanotube with a graphene sheet using a least-squares approach. Since we are comparing an essentially discrete not strictly axially symmetric surface with a continuous axially symmetric one, there is no unique procedure to do this. Here we adopt as the comparison surface from Baowan *et al* [1] to be that which is defined by the two central atomic locations, and the two midpoints between the two atoms at the end points on the graphene sheet and the carbon nanotube. In Baowan *et al* [1], the radius of the fixed part of the graphene sheet is

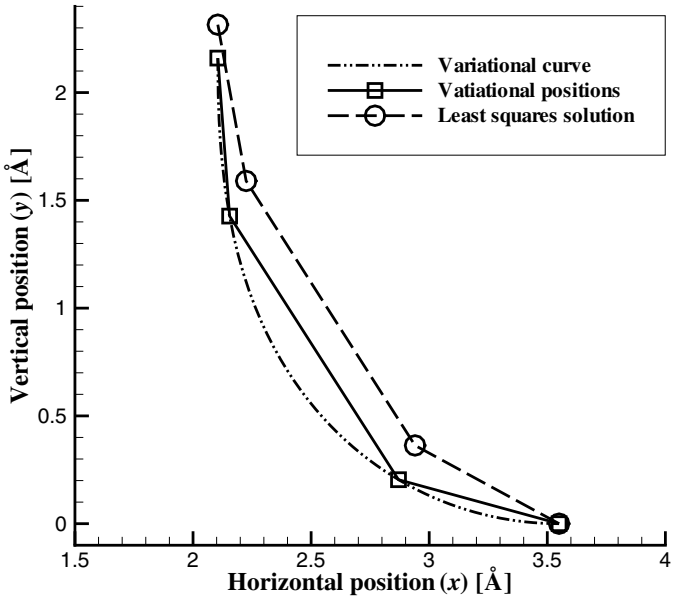

Figure 4. Comparison of the join shape for a (6,0) tube joining graphene using the variational and least-squares methods.

Table 2. Atomic positions for the variational method compared with the least-squares procedure for a (6,0) to graphene join.

Least squares		Variational			
x	y	x	y	Error (Å)	Parameter value ϕ
3.55	0	3.55	0	0	0
2.94	0.363	2.87	0.204	0.174	−0.409 792 50
2.225	1.59	2.155	1.427	0.177	−1.134 944 49
2.105	2.315	2.105	2.16	0.155	−1.445 179 78

3.55 Å, and the fixed part of the tube radius is taken to be 2.105 Å. It is a little more difficult to specify the arc length ℓ for this comparison since in the least-squares study, the join comprises three straight sections of lengths 0.71 Å, 1.42 Å and 0.735 Å. These sections sum to a total length of 2.865 Å. However, we cannot simply use this as a value for ℓ since it does not account for the curvature inherent in the variational solution. Therefore, we assume that the join curve will be approximately a quarter circle and we also assume that the longest straight section (1.42 Å) subtends an angle of $\pi/4$ radians at the centre of the circle. In this way, we may derive a more comparable arc length $\ell \approx 2.914$ Å. Using these values we derive a value $\mu = 0.4959$ and an attachment height $y_0 = 2.16$ Å which compares reasonably well with the figure for the least-squares approach which is $y_0 = 2.315$ Å, since it differs by only 0.155 Å or 6.7%. In figure 4, we graph the join shapes predicted by the variational and least-squares methods. Also shown in the figure are the assumed atomic locations for the variational approach which are denoted by squares that are joined by straight lines for comparison purposes. It can be seen from this figure that the y_0 height is similar in both cases, but the atomic locations which participate in the join as compared to those predicted by the least-squares method are not quite as accurate (see table 2). The third column of table 2 is the absolute distance between

the two predictions, while the fourth column gives the corresponding parameter value for ϕ. Despite this apparent discrepancy, the absolute error for the participating atomic positions is still within 0.18 Å of that predicted by the least-squares method.

6. Conclusions

In this paper, we propose a variational approach to determine the join between a carbon nanotube and a graphene sheet as an alternative procedure to the least-squares approach examined by Baowan *et al* [1]. The variational approach is based on the principle of minimizing the square of the curvature which in turn relates to the minimization of covalent bond energy. Analysis of the solution has identified the characteristic parameter $\mu = (x_0 - a)/\ell$ and three solution regimes. The first regime is when $2/\pi < \mu < 1$ and the curve is shallower than a quarter circle. The point $\mu = 2/\pi$ relates to the special case where the curvature is constant and the join curve is precisely a quarter circle. The second regime occurs for the range $\mu_0 < \mu < 2/\pi$, where μ_0 is given by equation (28). Here the curve is steeper than a quarter circle but still comprises only positive curvature. The point $\mu = \mu_0$ corresponds to the case when the curvature approaches zero at the end point $x = a$. The final regime applies for the range $-1 < \mu < \mu_0$ and corresponds to Model II when the join curve comprises both the positive curvature and negative curvature regions. A comparison with the results for a (6,0) and a graphene join using the least-squares and variational methods shows that the tube connect height y_0 is in good agreement (an absolute error of 0.155 Å), although the agreement in the atomic positions participating in the join is not quite as good but still within an absolute error of 0.18 Å. However, some disagreement is not entirely unexpected since we are effectively attempting to derive only two points from a continuous method and the procedure for determining the comparison surface is by no means unique.

Acknowledgments

The authors are grateful to the Australian Research Council for their support through the Discovery Project Scheme and the provision of an Australian Postdoctoral Fellowship for NT and an Australian Professorial Fellowship for JMH. The authors also wish to acknowledge Professor Andrejs Treibergs from the University of Utah for his many helpful comments.

References

[1] Baowan D, Cox B J and Hill J M 2007 Two least squares analyses of bond lengths and bond angles for the joining of carbon nanotubes to graphenes *Carbon* **45** 2972–80

[2] Cornell W D *et al* 1995 A second generation force field for the simulation of proteins, nucleic acids, and organic molecules *J. Am. Chem. Soc.* **117** 5179–97

[3] Li C and Chou T-W 2003 A structural mechanics approach for the analysis of carbon nanotubes *Int. J. Solids Struct.* **40** 2487–99

[4] Jin Y and Yuan F G 2003 Simulation of elastic properties of single-walled carbon nanotubes *Compos. Sci. Technol.* **63** 1507–15

[5] Natsuki T, Tantrakarn K and Endo M 2004 Effects of carbon nanotube structures on mechanical properties *Appl. Phys.* A **79** 117–24

[6] Zang J, Treibergs A, Han Y and Liu F 2004 Geometric constant defining shape transitions of carbon nanotubes under pressure *Phys. Rev. Lett.* **92** 105501

[7] Byrd P F and Friedman M D 1971 *Handbook of Elliptic Integrals for Engineers and Scientists* 2nd edn (Berlin: Springer)